Available online at www.sciencedirect.com
SCIENCE DIRECT
Journal of Sound and Vibration 296 (2006) 59–72
JOURNAL OF SOUND AND VIBRATION
www.elsevier.com/locate/jsvi

High-speed trains: Prediction of micro-pressure wave radiation from tunnel portals

A. Baron*, P. Molteni, L. Vigevano

Dipartimento di Ingegneria Aerospaziale, Facoltà di Ingegneria Industriale del Politecnico di Milano, Via La Masa, 34, 20156 Milan, Italy

Received 11 October 2004; received in revised form 14 November 2005; accepted 31 January 2006
Available online 23 May 2006

Abstract

Compression waves generated by trains entering a tunnel travel toward the opposite portal, where they are partly reflected back in the tunnel as expansion waves and partly radiated outside as *micro-pressure waves*. The intensity of the micro-pressure waves is related to the pressure gradient of the oncoming wave that, during its propagation within the tunnel, can either become steeper or smoother, according to the balance between viscous, thermal and nonlinear effects. Under the worst conditions, micro-pressure waves can become cause of concern producing noise and vibrations in the environment close to the tunnel exit.

Starting from the observation that pressure waves propagation in tunnels is mainly a one-dimensional (1D) phenomenon, this work presents a method capable of predicting the pressure disturbances radiated from tunnel portals based on the classical linear acoustic formulation by Kirchhoff, in which the source data are obtained by the solution of the unsteady quasi-1D equations of gas dynamics.

Comparisons with both full-scale and reduced-scale experiments about micro-pressure wave radiation are presented. The results show that the proposed, highly efficient method is able to capture the fundamental features of pressure waves propagation within tunnels as well as pressure radiation at their portals.

1. Introduction

The entry of a train in a tunnel generates compression and expansion waves whose intensity and gradient mainly depend on the train speed, blockage ratio (train to tunnel cross-section area ratio) and nose shape [1]. These waves propagate along the tunnel and are reflected at the tunnel ends, resulting in a strongly unsteady pressure field. The rapid and severe variation of pressure can cause discomfort to passengers travelling on trains and, under certain conditions, even the environment close to the tunnel portals can suffer from acoustic loads. These are produced by the radiation of micro-pressure waves, which are transmitted outside the tunnel when the compression wave generated by the entry of the train nose is reflected at the opposite portal. According to the literature on the subject [2–4], the disturbance caused by the micro-pressure waves is related to the maximum pressure gradient of the wave incident at a portal. This value, that is a measure of the

*Corresponding author. Tel.: +39 02 2399 8358; fax: +39 02 2399 8334.
E-mail address: arturo.baron@polimi.it (A. Baron).

0022-460X/$ - see front matter © 2006 Elsevier Ltd. All rights reserved.
doi:10.1016/j.jsv.2006.01.067

steepness of the wave front, results from a balance between friction forces and nonlinear effects, which all affect the properties of the nose pressure wave during its propagation along the tunnel: on one side, due to viscous effects, the amplitude of the wave is reduced and the width of its front spreads; on the other side the wave front tends to steepen, due to a propagation speed which is higher in higher pressure regions. As a consequence, severe micro-pressure waves, that are heard as noise (similar to a *sonic boom*) or vibrations of windows and structures in the neighborhood of the portal, can be cause of concern: to date, this has been reported only in Japanese railways, where slab track tunnels have been in use for a long time [5], but, more recently, it has become an important issue also in Europe, where new high-speed slab track lines are also under construction. The problem is less critical for ballast tracks, where the wave steepening may be strongly reduced or even absent [6,7].

The prediction of the impulsive pressure disturbances radiated from portals, as a consequence of the entry of a high-speed train into a tunnel, therefore requires the accurate reproduction of: (1) the generation of the compression wave by the train nose; (2) the pressure wave evolution during its propagation along the tunnel, accounting for viscous and nonlinear effects; (3) the strength and steepness of the disturbances transmitted into the environment outside the tunnel.

Different methods have been used for each of these stages. Basically, they can be divided into two different approaches: the first one consists in separating the problem of the internal flow from that of the external one; the second one considers the tunnel and the external environment as a single domain. Yoon and Lee [8] follow in their work the former approach and propose the linear formulation by Kirchhoff for the calculation of micro-pressure waves outside the tunnel while for the internal flow they consider different possibilities: (i) an acoustic monopole analysis, which has also been used, together with moving dipole sources, in Refs. [9,10]; (ii) a simplified analytical method of characteristics; (iii) the solution of the three-dimensional (3D) Euler equations, including moving meshes to represent the train motion (see also Ref. [11]). In the frame of the second approach described above, a two-dimensional (2D) plane/axisymmetric method based on the Euler equations has been developed by [12] to compute the complete pressure field inside and outside the tunnel.

Though 2D/3D flow models are more complete than one-dimensional (1D) generation/propagation models, especially in the entry phase where 3D effects are important, they require a great amount of computational resources that is not necessarily justified by the physics of the propagation of compression waves in a tunnel which is mainly a 1D phenomenon. In fact, the train–tunnel unsteady aerodynamics can be successfully described by a quasi-1D approximation of the physical problem, provided that local corrective models are adopted to better describe the regions where 3D effects become important, such as train nose and tail, tunnel cross-section variations and connections between tunnels and ducts. One of such 1D models [13–15] has been developed in the past decade to compute the unsteady, compressible flow induced by the transit of trains in complex tunnel nets. The obvious advantage of a 1D approach resides in its low computational cost, which allows to analyze complete, long tunnels or tunnel networks and to carry out parametric studies efficiently, while its drawback is that the reliability of its predictions partly depends on the availability of experimental data. These are required in order to assess the additional local models that take into account those 3D phenomena such as turbulent diffusion, wakes and separation that cannot be resolved directly. For this reason, the validation with experimental data or numerical results obtained through more general models is always recommended when 1D models are adopted.

On this ground, this work presents a method capable of predicting the pressure disturbances radiated from tunnel portals following the CFD/Kirchhoff approach of Yoon and Lee: the method couples the solution of the quasi-1D set of equations of gas dynamics for the internal flow with the classical linear acoustic formulation by Kirchhoff for the external one.

The paper is organized as follows: Section 2 describes both the numerical method adopted to compute the unsteady flow generated by the transit of trains in tunnels and the analytical formulation used to model the propagation of the pressure waves outside the tunnel portal. The influence of numerical (mesh size) and physical (friction) parameters on the solution is assessed in Section 3. In Section 4 the numerical method is applied to the prediction of micro-pressure waves radiation outside the tunnel in two experimental situations and the results are discussed. The method is then used in Section 5 to carry out a parametric study of the dependence of the amplitude of the micro-pressure waves with train speed, nose length and blockage ratio. Finally, Section 6 summarizes the main results and conclusions.

2. Physical and numerical models

The method for predicting pressure pulses emerging from the exit portal of a tunnel is obtained by combining a quasi-1D formulation for the internal flow and the Kirchhoff formulation for the external 3D pressure field. The equations of conservation of mass, momentum and energy, describing the unsteady, compressible flow of a gas are first solved to calculate the pressure transient within the tunnel. The solution at the tunnel exit is then used in the frame of the linear acoustic theory to predict the intensity of pressure disturbances radiated outside, at any given distance and location.

2.1. Flow inside the tunnel

The flow induced by the transit of high-speed trains in tunnels is resolved with a numerical tool based on a quasi-1D representation of the air flow and train motion described in Refs. [14,15], where full details on the physical models are given. Some additional details on the numerical method are described here.

The unsteady, quasi-1D flow of a viscous, compressible fluid is governed by the Navier–Stokes equations in which the variables are assumed to be uniform in each tunnel cross-section and therefore only depend on the axial coordinate. Considering the fact that viscous terms stem only from the interactions between the fluid and the train and tunnel walls, the governing equations may be written in a very general integral form for a varying control volume $\Omega(t)$ of surface $\Sigma(t)$ as

$$\frac{\mathrm{d}}{\mathrm{d}t}\int_{\Omega(t)} \mathbf{w}\,\mathrm{d}\Omega + \oint_{\Sigma(t)} \mathbf{f}\,\mathrm{d}\Sigma = \int_{\Omega(t)} \mathbf{s}\,\mathrm{d}\Omega, \tag{1}$$

where the vector of conservative variables $\mathbf{w}$, the vector of convective fluxes $\mathbf{f}$ and the source vector $\mathbf{s}$ are given by

$$\mathbf{w} = \begin{pmatrix} \rho \\ \rho u \\ E^t \end{pmatrix}, \quad \mathbf{f} = \begin{pmatrix} \rho u \\ \rho u^2 + p \\ (E^t + p)u + k\dfrac{\partial T}{\partial x} \end{pmatrix}, \tag{2}$$

$$\mathbf{s} = \begin{pmatrix} 0 \\ \dfrac{1}{A}\left[p\dfrac{\partial A}{\partial x} - C_{f_g}\dfrac{1}{2}\rho u|u|\mathscr{P}_g - C_{f_t}\dfrac{1}{2}\rho(u-V_t)|u-V_t|\mathscr{P}_t\right] \\ \dfrac{1}{A}\left[-pV_t\dfrac{\partial A}{\partial x} - C_{f_t}\dfrac{1}{2}\rho(u-V_t)|u-V_t|\mathscr{P}_t V_t\right] + \dot{Q} \end{pmatrix}, \tag{3}$$

with ρ air density, u air velocity, V_t train velocity, $E^t = \rho e + \frac{1}{2}\rho u^2$ total energy per unit volume, e internal energy per unit mass, p air pressure, T air temperature and k air thermal conductivity. The source vector $\mathbf{s}$ originates from: (1) the 1D approximation of the variations of the tunnel cross-section area $A(x,t)$ due to the tunnel geometry and to the presence of the moving trains; (2) the viscous contributions, where $\mathscr{P}$ is the perimeter of the cross-section, C_f is the skin friction coefficient, and subscripts g and t refer, respectively, to tunnel and train; (3) the thermal effects, where $\dot{Q}$ is the heat power per unit volume. The equations of state of polytropic ideal gases

$$p = \rho RT, \quad e = C_v T, \tag{4}$$

where C_v and R are, respectively, the specific heat at constant volume and the gas constant for air, are finally used to define the thermodynamic state and to balance the number of unknown quantities.

The spatial discretization of the domain is carried out by a cell-centered finite volume method. The train displacement implies the time and space variation of the cell volumes and interfaces areas. Hence, in the balance equations (1), $\Omega(t)$ is the instantaneous free volume obtained by subtracting the volume occupied by all the trains present in the considered section at any given time from the volume of each tunnel element. In the same way, the flux terms are computed by considering only the instantaneous free cross-sections of the tunnel.

The convective fluxes are discretized with a Jameson-like centered approach [16]. By approximating the integrals in Eq. (1) over the control volume $\Omega_j(t)$ as

$$\int_{\Omega_j(t)} \mathbf{w}\,\mathrm{d}\Omega = \Omega_j(t)W_j(t),$$

$$\oint_{\Sigma_j(t)} \mathbf{f}\,\mathrm{d}\Sigma = A_{j+\frac{1}{2}}(t)F_{j+\frac{1}{2}}(t) - A_{j-\frac{1}{2}}(t)F_{j-\frac{1}{2}}(t) = C_j(W_j;t),$$

$$\int_{\Omega_j(t)} \mathbf{s}\,\mathrm{d}\Omega = \Omega_j(t)S_j(W_j;t), \tag{5}$$

where

$$F_{j+\frac{1}{2}}(t) = \mathbf{f}\left(\frac{W_j + W_{j+1}}{2};t\right)$$

and $W_j(t)$ and $S_j(W_j;t)$ are the cell space average values of the unknowns and source vectors, the semi-discrete system of equations reads:

$$\frac{\mathrm{d}}{\mathrm{d}t}(\Omega_j W_j) = -C_j(W_j) + \Omega_j S_j(W_j), \tag{6}$$

where the explicit dependence on time has been dropped for conciseness. To avoid the spurious numerical oscillations, associated with the centered flux evaluation, system (6) is modified by adding a low-order numerical dissipation term $\Omega_j D_j(W_j)$ as

$$\frac{\mathrm{d}}{\mathrm{d}t}(\Omega_j W_j) = -C_j(W_j) + \Omega_j(S_j(W_j) + D_j(W_j)), \tag{7}$$

where $D_j(W_j)$ has the expression:

$$D_j(W_j) = \varepsilon(W_{j-1} - 2W_j + W_{j+1}),$$

being ε an empirical coefficient of the order of 0.1–0.2.

Time integration of the semi-discrete system (7) is carried out with an explicit five-stage Runge–Kutta time stepping scheme. To increase the stability interval with respect to standard Runge–Kutta algorithms, the convective and source terms of the residual are treated in different ways [17]: while the convective terms is continuously updated, the source term is not. Writing

$$B_j(W_j) = S_j(W_j) + D_j(W_j)$$

and

$$W_j^n = W_j(t^n)$$

the multi-stage time stepping scheme is formulated as

$$W_j^0 = W_j^n,$$

$$W_j^k = W_j^0 + \alpha_k \Delta t(-C_j^{k-1} + B_j^{k-1}) \quad \text{for } 1<k<K_s,$$

$$W_j^{n+1} = W_j^{K_s}, \tag{8}$$

where the superscript k denotes the kth stage, $K_s = 5$ being the total number of steps and

$$C_j^k = C(W_j^k), \quad B_j^0 = \beta_1 B(W_j^0),$$

$$B_j^k = \beta_{k+1} B(W_j^k) + (1-\beta_{k+1})B_j^{k-1}.$$

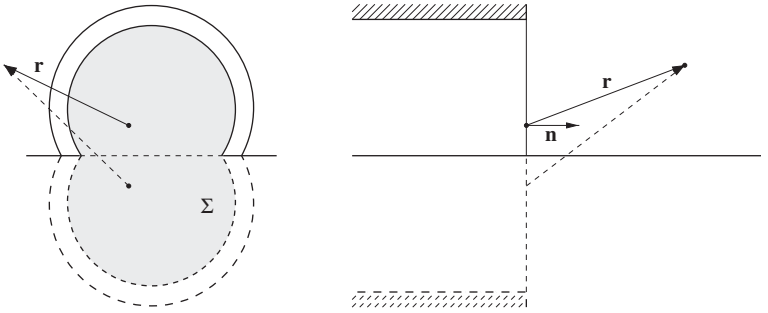

Fig. 1. Configuration of the integration surface with the image source accounting for the presence of the ground.

The coefficients α_k and β_k are chosen to maximize the stability region in order to allow larger time steps. In theory, a maximum value of CFL = 4 is permitted by the vectors of coefficients

$$\alpha = (\tfrac{1}{4}, \tfrac{1}{6}, \tfrac{3}{8}, \tfrac{1}{2}, 1),$$

$$\beta = (1., 0., 0.56, 0., 0.44). \tag{9}$$

2.2. Pressure field outside the tunnel

The pressure perturbation at a point $\mathbf{x}$ outside the tunnel portal and at time t, according to the Kirchhoff formulation, is given by [18]

$$p(\mathbf{x};t) = \frac{1}{4\pi}\int_{\Sigma}\left[\frac{p(\mathbf{x}';t')}{|\mathbf{r}|^3}\,\mathbf{r}\cdot\mathbf{n} - \frac{1}{|\mathbf{r}|}\frac{\partial p}{\partial n}\bigg|_{(\mathbf{x}';t')} + \frac{\mathbf{r}\cdot\mathbf{n}}{c_0|\mathbf{r}|^2}\frac{\partial p}{\partial t'}\bigg|_{(\mathbf{x}';t')}\right]\mathrm{d}\Sigma, \tag{10}$$

where (see Fig. 1) $\mathbf{r} = \mathbf{x} - \mathbf{x}'$ is the radiation vector, $\mathbf{x}'$ is a generic point on the surface Σ, $\mathbf{n}$ is the unit normal vector of the integration surface Σ, $t' = t - |\mathbf{r}|/c_0$, where c_0 is the external speed of sound. Pressure p and its derivatives are calculated from the 1D numerical solution at the tunnel exit and at time t'. Both time and space derivatives are approximated by second-order backwards finite differences.

In order to take into account the presence of the ground, an image source has been considered: i.e. the integration surface Σ is the sum of the tunnel exit cross-section and its reflected image with respect to the ground plane.

3. Analysis of mesh size and skin friction coefficient dependence

The reliability of the 1D model has been widely tested during the years, through comparison with analytical solutions for compressible flows, such as shock tube or acoustic wave propagation [15], as well as with published experimental data obtained for various railway tunnels and train configurations [1,19,20]. From past experience, when the amplitude of the pressure waves inside the tunnel is of interest, a good compromise between accuracy and efficiency is achieved by selecting a dimension of the mesh size around one-tenth of the tunnel hydraulic diameter. However, the mesh size shows to have very little influence on the predicted amplitude of the pressure waves. The skin friction coefficient, on the contrary, strongly affects the amplitude of the waves: values ranging from 0.005 to 0.040 are used, depending on the actual degree of roughness, the presence of refuges and ballast. The effects of unsteady friction phenomena [21], are not considered in the present model.

When micro-pressure wave radiation at tunnel portals has to be simulated, a more accurate prediction of pressure gradients is required in order to capture the correct evolution of the wave fronts inside the tunnel. This suggested to evaluate the influence of both grid spacing and friction coefficient on the numerical

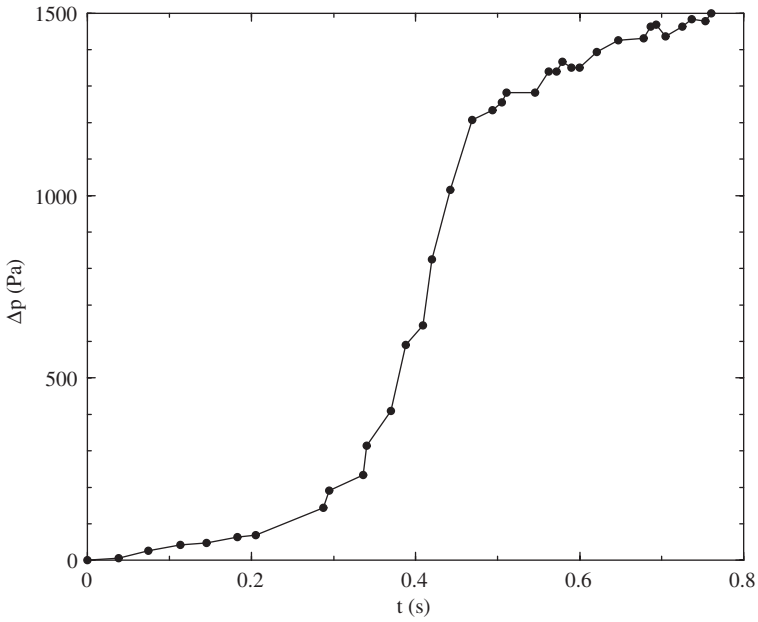

Fig. 2. Measured pressure history [22] 103 m from the tunnel entrance used as boundary condition in the numerical test.

solutions. Thermal effects have not been considered in the present study, since they may be considered negligible in absence of a fire accident scenario.

The experimental work by Mashimo et al. [22], in which pressure measurements were recorded in three different sections of a tunnel of the Japanese Shinkansen line (103, 3261 and 6073 m from the entrance), has been used as a reference. The numerical prediction of the pressure transient has been carried out by imposing the experimental pressure history of Fig. 2, gathered 103 m from the beginning of the tunnel, as inlet boundary condition. At each time step, pressure is linearly interpolated from the experimental time history and then used to calculate the boundary values of the conservative variables assuming isentropic relations. No fitting of the irregular boundary data has been performed, since the adopted numerical viscosity is adequate to prevent oscillations. The results of the numerical simulations have then been compared with experimental data at the two downstream sections.

Different tests have been performed with grid spacings of one-tenth, one-twentieth and one-fortieth of the hydraulic diameter of the tunnel and with skin friction coefficients equal to 0.01, 0.02 and 0.04. Adiabatic walls and standard initial air conditions have been considered. As expected, the sensitivity analysis confirms that the mesh size has no effect on the amplitude of the pressure waves, while it strongly influences the prediction of the front steepness (Figs. 3 and 4) which can be either under- or overestimated. However, the results of Fig. 5 show a tendency to grid independence, indicating that convergence is being approached. The unavoidable dispersion of experimental data introduces a certain degree of arbitrariness in the evaluation of the maximum time derivative of pressure, which makes a quantitative comparison of these results difficult. Nevertheless, the use of meshes finer than one-tenth of the tunnel hydraulic diameter is recommended when the steepness of wave fronts is of interest. As far as friction forces are concerned, their effect is to reduce the wave amplitude: the higher the forces, the lower the amplitude and this, of course, has also a slight effect on the gradient.

4. Numerical simulation of micro-pressure wave radiation

In the present section, the numerical method outlined in Section 2 is applied to the simulation of micro-pressure wave radiation for two test cases for which experimental data have been published. The first one concerns the full-scale measurements in the Terranuova Le Ville tunnel of the Italian railway high-speed line

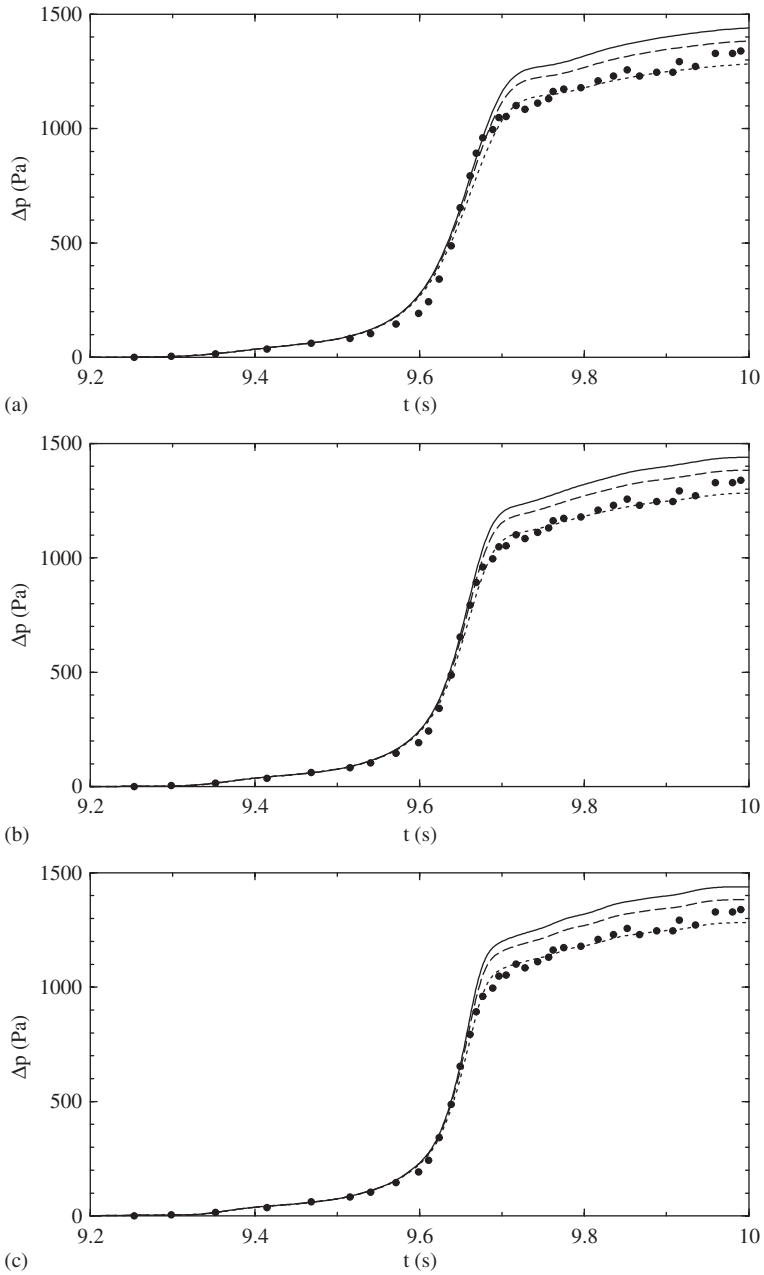

Fig. 3. Pressure histories 3261 m from the tunnel entrance. Mesh spacing in fractions of the tunnel hydraulic diameter: (a) one-tenth; (b) one-twentieth; (c) one-fortieth. (•) Experimental data [22]; (—) $C_{fg} = 0.01$; (– –) $C_{fg} = 0.02$; (· · ·) $C_{fg} = 0.04$.

linking Firenze to Roma [23]. The second one is a reduced-scale experiment carried out at the NLR laboratory in The Netherlands [24]. On the basis of the sensitivity analysis of Section 3, all the simulations have been performed with a mesh size Δx = one-twentieth of the tunnel hydraulic diameter. Moreover, the CFL number used in this work is 2.

The full-scale measurements of the pressure transients induced by ETR 500 trains in the Terranuova Le Ville tunnel are used as a first test case. The tunnel length is 2701 m and the area of the cross-section is 69 m^2, except for a length of 121 m near the South portal, where the area is 116 m^2. Two different conditions are examined: in the first one, a single train enters the South portal at 221 km/h, while in the second one two

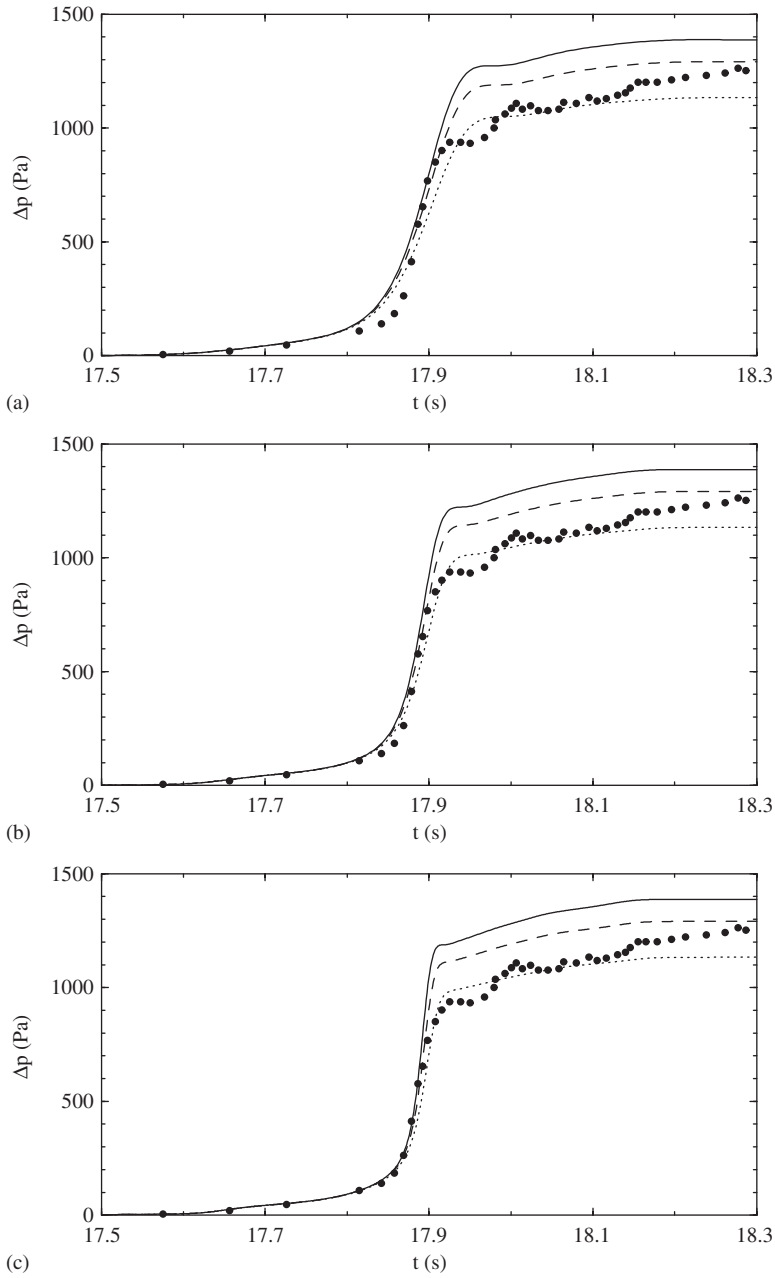

Fig. 4. Pressure histories 6073 m from the tunnel entrance. Mesh spacing in fractions of the tunnel hydraulic diameter:(a) one-tenth; (b) one-twentieth; (c) one-fortieth. (•) Experimental data [22]; (—) $C_{f_g} = 0.01$; (– –) $C_{f_g} = 0.02$; (· · ·) $C_{f_g} = 0.04$.

parallel trains enter simultaneously at 230 km/h (the total blockage in the latter case is 0.31). In both cases, the radiated disturbances are recorded 30 m far from the exit, at a point located on the tunnel axis.

The complete propagation of the wave in the tunnel has been simulated. The initial wave is generated by the entry of the ETR 500 train, whose specific parameters have been tuned and validated in previous works through comparison with experimental data [20]: the train head and tail coefficients defined in [15] are, respectively, $C_{\text{head}} = 1.001$ and $C_{\text{tail}} = 0.995$. Based on previous experience, the skin friction coefficient adopted for the Terranuova tunnel is 0.02.

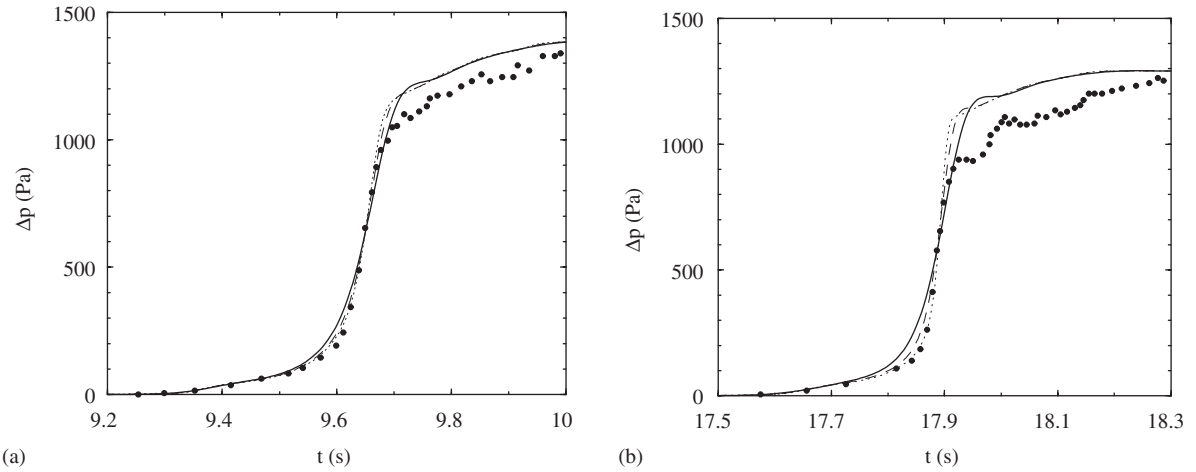

Fig. 5. Pressure histories (a) 3261 m; (b) 6073 m from the tunnel entrance. $C_{fg} = 0.02$. (•) Experimental data [22]. Mesh spacing in fractions of the tunnel hydraulic diameter: (—) one-tenth; (––) one-twentieth; (···) one-fortieth.

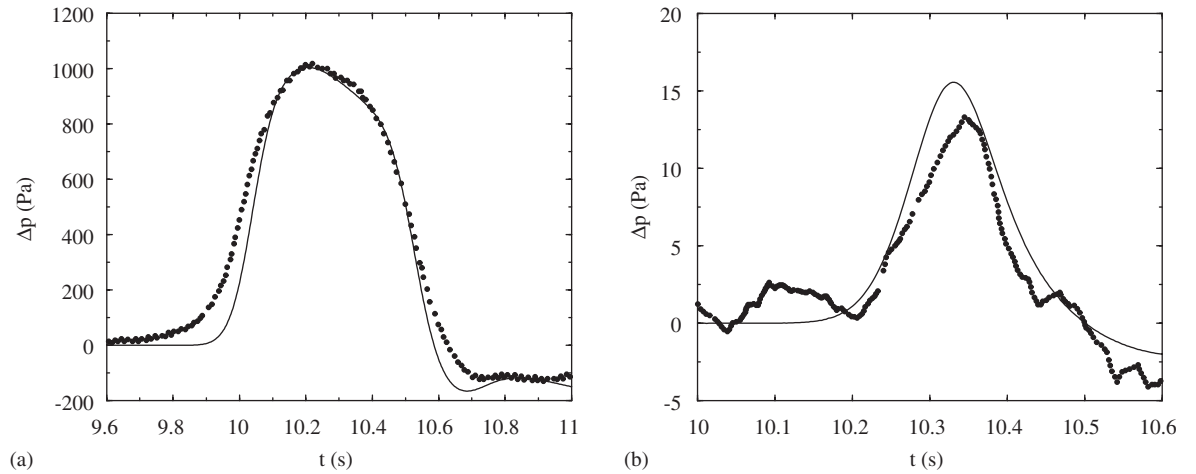

Fig. 6. Terranuova single-train full-scale test case: train speed 221 km/h; blockage ratio 0.155. (a) Pressure history at point 80 m from tunnel exit; (b) micro-pressure wave 30 m far from tunnel exit and on the tunnel axis. (•) Experimental data [23]; (—) numerical prediction.

While the amplitude of the oncoming pressure wave is reproduced quite well in the case of a single train, as Fig. 6(a) shows, the maximum gradient is somewhat higher than the experimental one. As a consequence, the amplitude of the predicted wave radiated outside is also higher (Fig. 6(b)). The numerical result for the two parallel trains case, reported in Fig. 7(a), shows a slightly higher amplitude of the oncoming wave with respect to measurements, possibly due to real 3D entry effects that are stronger than the modelled ones. However, this has little influence on the computed micro-pressure wave shown in Fig. 7(b), since the amplitude has a lower effect on the radiated wave than the gradient has.

As far as the reduced-scale experiments are concerned, the tunnel model has a rectangular cross-section 40 mm high and 97 mm wide and its total length is 7.64 m. The axisymmetric train model has a diameter of 20 mm and is 2.34 m long. The resulting blockage ratio is 0.081. The length of the train head is 70 mm. The comparison is made with three different tests in which only the train speed is varied, the values being 300, 350 and 380 km/h. Micro-pressure waves are recorded in a point located 20 mm above the tunnel ground and 120 mm far from the tunnel exit. Time histories of pressure inside the tunnel are also monitored in different sections. Geometrical parameters have been chosen according to the experimental setup and a tunnel skin

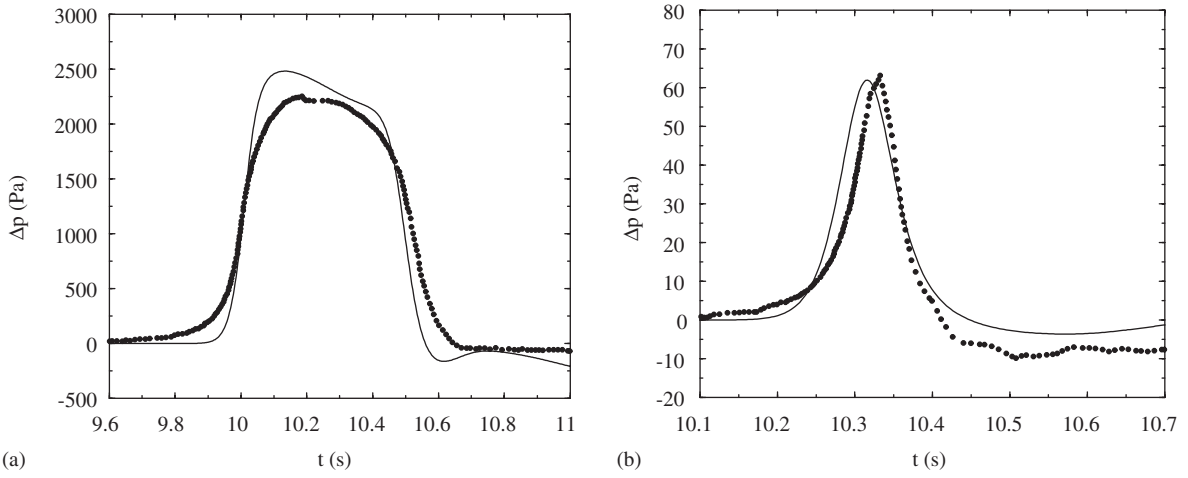

Fig. 7. Terranuova two-train full-scale test case: train speed 230 km/h; blockage ratio 0.31. (a) Pressure history at point 80 m from tunnel exit; (b) micro-pressure wave 30 m far from tunnel exit and on the tunnel axis. (•) Experimental data [23]; (—) numerical prediction.

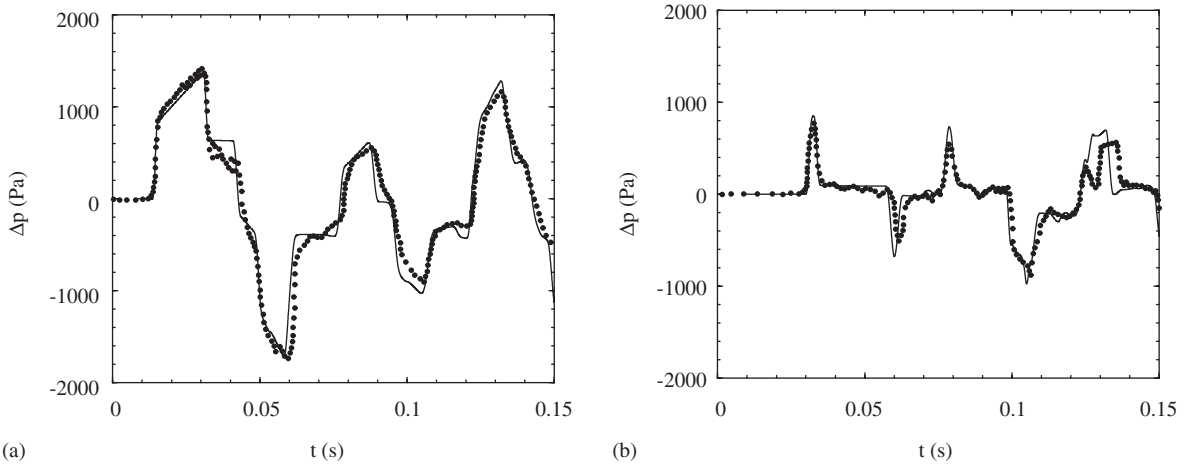

Fig. 8. NLR reduced-scale test case: train speed 300 km/h; blockage ratio 0.081. (a) Pressure history at point 1.868 m from tunnel entrance; (b) pressure history at point 7.227 m from tunnel entrance. (•) Experimental data [8]; (—) numerical prediction.

friction coefficient 0.01 has been adopted as a compromise between the relatively smooth surfaces involved and possible low Reynolds number effects.

Figs. 8(a) and (b) show the pressure time-history in two different sections inside the tunnel, 1.868 and 7.227 m from the tunnel entrance, respectively, obtained with a train speed of 300 km/h. The first pressure wave, generated by the train entering the tunnel, and the overall curve patterns are in very good agreement with the experimental data. Only a small discrepancy in the propagation speed of the reflected waves can be observed in both figures. This speed is dependent on the temperature that, in the experimental test, is influenced by the gas expansion in the pneumatic launching device, as underlined by the authors of the cited paper. This feature has however not been taken into account because it has no effect on the train nose pressure wave first arriving at the tunnel exit.

In the point closer to the tunnel entrance (Fig. 8(a)) the amplitude of the predicted initial wave (at time 0.015 s) is slightly smaller than the experimental one, while the pressure rate of change in the time interval between 0.015 and 0.031 s (essentially due to the train skin friction) is almost identical. By comparing Fig. 8(b) (approximately at time 0.03 s) to Fig. 8(a), it can also be noted that the amplitude of the computed nose

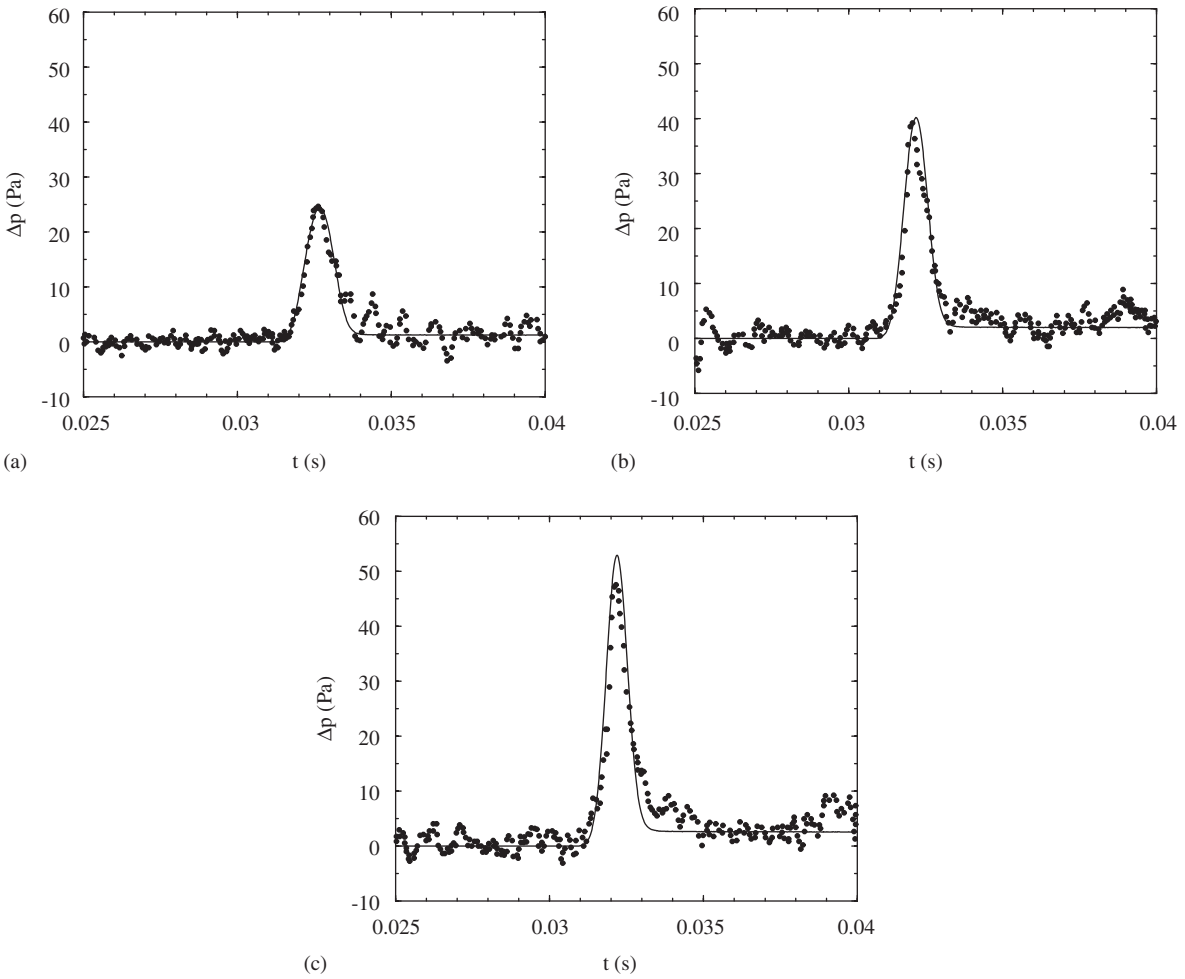

Fig. 9. NLR reduced-scale test case: micro-pressure wave 20 mm above ground and 120 mm far from tunnel exit; blockage ratio 0.081. Train speed: (a) 300 km/h; (b) 350 km/h; (c) 380 km/h. (•) Experimental data [8]; (—) numerical prediction.

compression wave reduces less than the experimental one, which can be attributed to higher dissipation effects in the experimental facility. Nevertheless, this is assumed to have little effect on the intensity of the radiated disturbances that, as mentioned, are known to depend almost only on the gradient of the pressure front and not on its amplitude. As a matter of fact, Figs. 9(a)–(c) show that, outside the tunnel, both the amplitude and the period of the micro-pressure waves at 120 mm are in good agreement with the experiments in all of the analyzed conditions, which confirms the correctness of the assumptions.

Furthermore, it has to be remarked that the time required for each simulation is something like 2 min of CPU on a personal computer Pentium IV 1.7 GHz. This fact allows to carry out parametric studies on different configurations very efficiently and makes this method a useful tool for preliminary design.

5. Parametric study

The amplitude of the micro-pressure waves is known to depend on the train speed, blockage ratio and train nose length, which all affect the steepness and amplitude of the oncoming pressure wave. In the same way, the skin friction of both train and tunnel, as well as the use of suitably located shafts, can also alter the intensity of the radiated pulses. The number of parameters involved in the examined phenomenon is such that in the preliminary stage of a design, a comprehensive parametric analysis can only be performed by using relatively simple tools such as the one that is here proposed.

As an example, we refer again to the single-train case of Terranuova described in Section 4, in order to assess the influence of some of the above mentioned parameters. The analysis is carried out varying one parameter at the time. The tunnel geometry is kept constant when the blockage ratio is varied and the train is

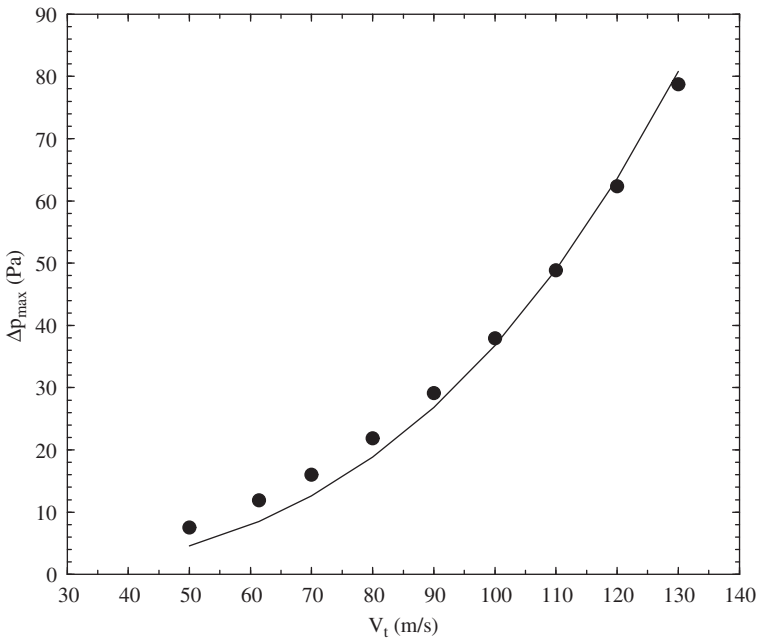

Fig. 10. Effect of the train velocity V_t on the maximum amplitude of the micro-pressure waves. Blockage ratio = 0.155, nose length = 4.4 m. (•) Numerical predictions; (—) curve fitting $\Delta p \propto V_t^3$.

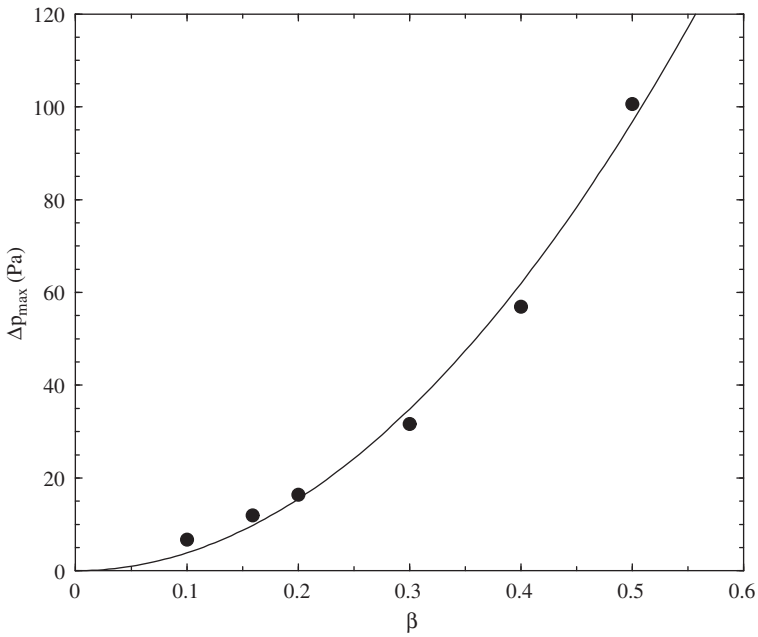

Fig. 11. Effect of the blockage ratio β on the maximum amplitude of the micro-pressure waves. Train speed = 61.4 m/s, nose length = 4.4 m. (•) Numerical predictions; (—) curve fitting $\Delta p \propto \beta^2$.

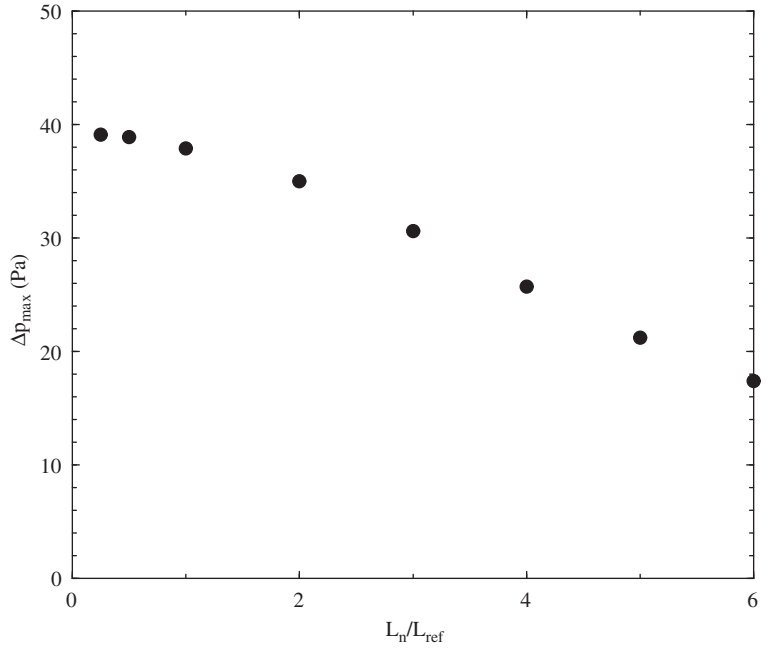

Fig. 12. Effect of the train nose length L_n on the maximum amplitude of the micro-pressure waves. Train speed = 100 m/s, blockage ratio = 0.155, L_{ref} = 4.4 m (ETR 500 nose).

scaled accordingly. The influence of the train nose length is analyzed at a train speed (100 m/s) higher than in the reference case, to enhance the amplitude of the pressure waves.

Fig. 10 shows that the increase of the micro-pressure wave amplitude with train velocity agrees with results for relatively short tunnels, where a dependence with the cube of the train speed is expected. The need of finding countermeasures to reduce the pressure pulses when high speeds are to be attained is confirmed.

A generally adopted solution to minimize the disturbances is to keep the blockage ratio as low as it is allowed by the need to limit tunnel construction costs. The influence of the blockage ratio on micro-pressure wave intensity is reported in Fig. 11: for engineering purposes, a quadratic adjustment of the computed data is a reasonable approximation of the dependence of the wave intensity on blockage ratio.

Great efforts are also dedicated to the design and optimization of the shape of the train head. In fact, though the train speed and blockage ratio determine the amplitude of the nose compression wave, the nose shape is the main responsible for its initial gradient. Fig. 12 shows how the relative nose length (with respect to the standard ETR 500 nose) influences the radiated disturbances. Though very long train noses are not realistic, the same attenuating effect can be obtained by means of flared portals or tunnel hoods.

6. Conclusions

A simple, numerical tool has been developed for the prediction of the micro-pressure waves radiating from railway tunnel portals, by coupling two different, complementary flow models for the internal and external flow domains. The approach has the advantage of taking into account the very peculiar physical aspects of each single flow domain, which strongly differ each other, while allowing a maximum simplification of each separate model. Accordingly, viscous and nonlinear effects are retained in the internal flow model, while a quasi-1D approach is adopted with almost no loss of information. On the contrary, three-dimensionality is fully preserved in the external field, while a linear, acoustic approach is absolutely acceptable.

Comparison of the predicted radiation of micro-pressure waves with both full-scale as well as reduced-scale measurements confirms the capability of the numerical tool to capture the fundamental features of the phenomenon. Results comparable to those of 3D internal flow models are obtained with a fraction of the

computational time, which makes the present method a useful tool in the preliminary analysis of various train and tunnel configurations.

References

[1] R.G. Gawthorpe, C.W. Pope, The measurement and interpretation of transient pressures generated by trains in tunnels, *Proceedings of the Second International Symposium on the Aerodynamics and Ventilation of Vehicle Tunnels*, Cambridge, UK, 1976, pp. 35–54.

[2] S. Ozawa, Studies of micro-pressure wave radiated from a tunnel exit. Technical Report 1121, Railway Technical Research Institute, Japan, 1979 (in Japanese).

[3] S. Ozawa, T. Maeda, T. Matsumura, K. Uchida, H. Kajiyama, K. Tanemoto, Countermeasures to reduce micro-pressure waves radiating from exits of Shinkansen tunnels, *Proceedings of the Seventh International Conference on the Aerodynamics and Ventilation of Vehicle Tunnels*, Brighton, UK, 1991, pp. 253–266.

[4] R.S. Raghunathan, H.D. Kim, T. Setoguchi, Aerodynamics of high-speed railway train, *Progress in Aerospace Sciences* 38 (2002) 469–514.

[5] S. Ozawa, T. Uchida, T. Maeda, Reduction of micro-pressure wave radiated from tunnel exit by hood at tunnel entrance, Technical Report 19 n. 2, Railway Technical Research Institute, Japan, 1978.

[6] S. Ozawa, K. Murata, T. Maeda, Effect of ballasted track on distortion of pressure wave in tunnel and emission of micro-pressure wave, *Proceedings of the Ninth International Conference on the Aerodynamics and Ventilation of Vehicle Tunnels*, Aosta Valley, Italy, 1997, pp. 935–947.

[7] A.E. Vardy, J.M.B. Brown, Influence of ballast in wave steepening in tunnels, *Journal of Sound and Vibration* 238 (4) (2000) 595–615.

[8] T.S. Yoon, S. Lee, Efficient prediction methods for the micro-pressure wave from a high-speed train entering a tunnel using the Kirchhoff formulation, *Journal of Acoustical Society of America* 110 (5) (2001) 2379–2389.

[9] M.S. Howe, On Rayleigh's computation of the 'end correction', with application to the compression wave generated by a train entering a tunnel, *Journal of Fluid Mechanics* 385 (1999) 63–78.

[10] M.S. Howe, M. Iida, T. Fukuda, T. Maeda, Theoretical and experimental investigation of the compression wave generated by a train entering a tunnel with flared portal, *Journal of Fluid Mechanics* 425 (2000) 111–132.

[11] K. Pahlke, Application of the standard aeronautical CFD method FLOWer to ETR 500 tunnel entry. *Proceedings of the TRANSAERO—A European Initiative on Transient Aerodynamics for Railway System Optimisation*, *Notes on Numerical Fluid Mechanics and Multidisciplinary Design*, Vol. 79, Springer, Berlin, 2002, pp. 217–224.

[12] K. Ehrendorfer, M. Reiterer, H. Sockel, Numerical investigation of the micro pressure wave. *Proceedings of the TRANSAERO—A European Initiative on Transient Aerodynamics for Railway System Optimisation*, *Notes on Numerical Fluid Mechanics and Multidisciplinary Design*, Vol. 79, Springer, Berlin, 2002, pp. 321–341.

[13] A. Baron, M. Arra, Transient flow prediction in railway tunnels, *Proceedings of the Royal Aeronautical Conference on Vehicle Aerodynamics*, University of Technology, Loughborough, UK, 1994, pp. 15.1–15.12.

[14] A. Baron, F. Losi, F. Orso, Simulazione numerica di fenomeni aerodinamici prodotti da treni ad alta velocità in tunnel di forma complessa, *Ingegneria Ferroviaria* 7 (1996) 3–19.

[15] A. Baron, M. Mossi, S. Sibilla, The alleviation of the aerodynamic drag and wave effects of high-speed trains in very long tunnels, *Journal of Wind Engineering and Industrial Aerodynamics* 89 (2001) 365–401.

[16] A. Jameson, W. Schmidt, E. Turkel, Numerical solutions of the Euler equations by finite volume methods using Runge–Kutta time-stepping schemes, *Proceedings of the AIAA Fifth Computations Fluid Dynamics Conference*, 1981, pp. 81–1259.

[17] A. Jameson, Time integration methods in computational aerodynamics, *Proceedings of the 2003 AFOSR Workshop on Advances and Challenges in Time-integration of PDEs*, Providence, RI, 2003, pp. 249–266.

[18] A. Pierce, *Acoustics—An Introduction to its Physical Principles and Applications*, Acoustical Society of America, Woodbury, New York, 1991.

[19] H. Glöcke, P. Pfretzschner, High speed tests with ICE/V passing through tunnels and the effect of sealed coaches on passenger comfort, *Proceedings of the Sixth International Symposium on the Aerodynamics and Ventilation of Vehicle Tunnels*, Durham, UK, 1988, pp. 23–44.

[20] G. Mancini, A. Malfatti, Full scale measurements on high-speed train ETR 500 passing in open air and in tunnels of Italian high-speed line. *Proceedings of the TRANSAERO—A European Initiative on Transient Aerodynamics for Railway System Optimisation*, *Notes on Numerical Fluid Mechanics and Multidisciplinary Design*, Vol. 79, Springer, Berlin, 2002, pp. 101–122.

[21] A.E. Vardy, J.M.B. Brown, Transient, turbulent, smooth pipe friction, *Journal of Hydraulic Research* 33 (4) (1995) 435–456.

[22] S. Mashimo, E. Nakatsu, T. Aoki, K. Matsuo, Attenuation and distortion of a compression wave propagating in a high-speed railway tunnel, *JSME International Journal Series B—Fluids and Thermal Engineering* 40 (1) (1997) 51–57.

[23] M. Reiterer, K. Ehrendorfer, H. Sockel, Experimental investigation of the micro pressure wave. *Proceedings of the TRANSAERO—A European Initiative on Transient Aerodynamics for Railway System Optimisation*, *Notes on Numerical Fluid Mechanics and Multidisciplinary Design*, Vol. 79, Springer, Berlin, 2002, pp. 290–301.

[24] T.S. Yoon, S. Lee, J.H. Hwang, D.H. Lee, Prediction and validation on the sonic boom by a high-speed train entering a tunnel, *Journal of Sound and Vibration* 247 (2) (2001) 195–211.